Microwave Review
July 2024, Vol. 30, No. 1, pp. 23-28
DOI: 10.18485/mtts_mr.2024.30.1.4

Design of X/Ku and K Band Flexible Cloud-Fractal Wideband Antenna with Bandwidth Estimation Using CMA

Bashar Bahaa Qas Elias, Mushtaq Ahmed Alqaisy, Ping Jack Soh

Abstract – **This paper proposes a new cloud-shaped fractal patch antenna with compact dimensions of 15 mm × 15 mm (0.85 λg × 0.85 λg) that will help achieve a wide bandwidth of up to 11.3 GHz. Here, λg represents the operating wavelength specified at the lower frequency (9.01 GHz) of the obtained band. Additionally, the lower frequency (*Lf*) variability within the obtained band is estimated using the characteristic mode analysis (CMA) technique at each iteration of the proposed fractal antenna. The simulated design demonstrates its potential application in the X, Ku, and K bands, making it suitable for various applications, including satellite communication and military use. The antenna employs Kapton polyimide as the substrate, with a dielectric constant of 3.5 and a thickness of 0.11 mm. The simulated -10 dB antenna exhibits peak gains of 4 dBi and 5 dBi. The radiation pattern and antenna efficiency are also analysed. All simulations are conducted using the FEKO simulator software. The antenna is fabricated and measured for verification, with the experimental results showing a satisfactory agreement with the simulation.**

Keywords – **Fractal antenna, CMA, bandwidth, lower frequency, gain.**

I. INTRODUCTION

Usually, traditional antennas have operated at a single frequency. Still, with the fast development of present day modern wireless communication systems and system applications, a wider bandwidth antenna is needed, which is why it has become the attention of many researchers [1-6]. There are numerous demands for Microstrip patch antennas in radar and space satellite communication applications because its low profile, mechanical robustness, relative compactness and lightweight, and double frequency operation. IEEE specifies the X/Ku Band as 8 to 12 GHz and 12 to 18 GHz, respectively. The X Band frequency band demands a rapid, secure satellite communication system.

Characteristic mode analysis (CMA) has been found to be a very useful tool for developing antenna structures. The CMA theory was introduced in [7], and since then, an expansion of this theory has been presented in [8] and [9]. Among its features, such as modal significance (MSn), eigenvalue (λn), and characteristic angle (βn), they allow it to depict modes as well as individual current flows. Thus, from an engineering perspective, CMA can provide sets of orthogonal current characteristics of conductive bodies; literally speaking, these are only related to the structure –size– frequency of operation of the antenna. This allows CMA to provide physical insights into antenna radiation, hence improving their comprehension of the structure thus allowing more efficient antenna design, synthesis, and optimization to occur [10] [11]. A fractal antenna is an improved version of one that uses a fractal, self-similar design in order to optimize effective length or enhance material perimeter. These fractal antennas are also known as multilevel and space filled curves. It offers universal wideband antenna technology suited for building communication applications [12-13]. Furthermore, fractal antennas provide distinct improvements to the antennas. These advantages include increased bandwidth, multiband capabilities, and reduced size load. A fractal antenna exhibits significantly different from traditional antenna designs in terms of its response. It has the ability to use with good-to-excellent performance at multiple frequencies simultaneously. Typically, standard antennas must be "cut" for the frequency at which they are to be used and hence only work well at that frequency. The fractal antenna is thus a good choice for wideband and multiband applications. Furthermore, the antenna's fractal nature reduces its size without using components such as inductors or capacitors.

Wearable antennas are commonly used to support wireless communication in such technological gadgets. Since they made of flexible materials, these antennas can be worn on different body parts such as the chest, wrist, head, and more. This allows for the sensing and monitoring of human characteristics such as heart rate [14]. Furthermore, flexible materials with low relative permittivity, like as textiles, have the potential to expand antenna bandwidth and reduce surface wave losses [15]. In this study, a new cloud-shaped fractal antenna is designed with a 0.11 mm high dielectric material substrate with bandwidths of 11.3 GHz (9.01 GHz–20.33 GHz) and 4 dBi, 5 dBi peak gain.

The paper is structured as follows: first, the proposed antenna is described in detail, followed by a simulation and a test of its performance in free space. The lowest frequency estimate based on the CMA approach is discussed in Section 4. Finally, Section 5 summarizes this paper with a conclusion.

Article history: Received July 21, 2023; Accepted February 20, 2024.

Bashar Bahaa Qas Elias is with the Department of Information and Communication Engineering, College of Information Engineering, Al-Nahrain University, Jadriya, Baghdad, Iraq, E-mail: bashar.bahaa@nahrainuniv.edu.iq.

Mushtaq Ahmed Alqaisy is with the Al-Iraqia University, College of Engineering, Computer Engineering Department, Baghdad, Iraq, E-mail: dr.mushtaq@aliraqia.edu.iq

Ping Jack Soh is with the Centre for Wireless Communications (CWC), University of Oulu, P.O. Box 4500, 90014 Oulu, Finland, E-mail: pingjack.soh@oulu.fi

II. ANTENNA CONFIGURATION

The main structure of the proposed fractal antenna is shown in Fig.1. The optimal geometrical parameters of the proposed antenna are obtained using FEKO full-wave electromagnetic simulator software based on the method of moments (MoM). It is printed on Kapton polyimide with a dielectric constant (εr) of 3.5, thicknesses of 0.11 mm, and a loss tangent (tan δ) of 0.045. This flexible material is easy to fabricate and stable in usage. They have mechanical stability, a tight dielectric constant, thickness control, and low moisture absorption. Shortly, the cloud shape fractal antenna consists of a set of elliptical shapes with radii $R1$ and $R2$ in iteration 1, $R3$ and $R4$ in iteration 2, and $R5$ and R6 in iteration 3. At the last stage of design, the ellipse shapes are arranged as a cloud shape. The total dimensions of the antenna are about 15 × 15 mm, and it is fed by a coplanar waveguide (CPW). Variations in the gap between the CPW and the microstrip feedline can cause a significant shift in antenna impedance matching. Therefore, it is crucial to precisely calculate the distance between the feed and ground plane, which is determined to be 0. 15 mm.

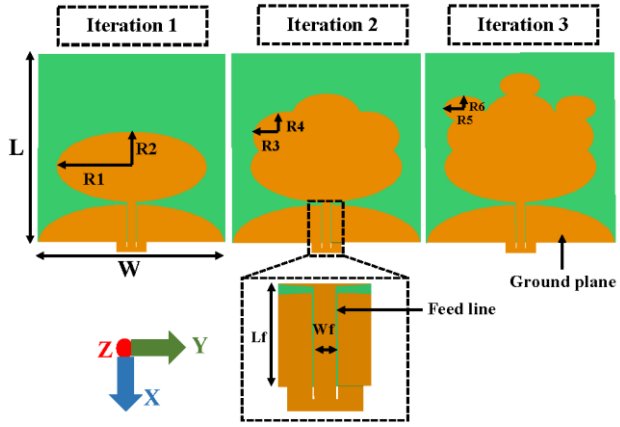

Fig.1. Configuration of the cloud fractal antenna. L = 15 mm, W = 15 mm, $R1$ = 6 mm, $R2$ = 2.8 mm, $R3$ = 2.8 mm, $R4$ = 2 mm, $R5$ = 1.6 mm, $R6$ = 1 mm, Lf = 4.4 mm, Wf = 0.7 mm

The subsequent passage outlines the step-by-step procedure: i) Print the fractal patch structure onto white paper, ensuring it matches the precise dimensions to prevent any deformation or movement during the integration process with the patch-substrate, as depicted in Fig. 2. (a). ii) Adhere this paper onto a larger piece of pliant conductive material exceeding the size of the patch, as illustrated in Fig. 2. (b). iii) Carefully use scissors and a blade to meticulously carve out the patch and ground plane configurations on the substrate, as shown in Fig. 2. (c). iv) Position these planes on the front side of a Kapton film substrate and securely bond the Sub Miniature Version A (SMA) connector to the feed line using silver epoxy, enabling the excitation as exemplified in Fig. 2. (d).

In Fig. 3, the process of designing the proposed fractal antenna and utilizing the CMA (Characteristics Mode Analysis) and MoM (Method of Moments) methods for antenna analysis is succinctly illustrated. This comprehensive approach allows for a thorough examination of the antenna's performance and characteristics, ensuring optimal design and functionality.

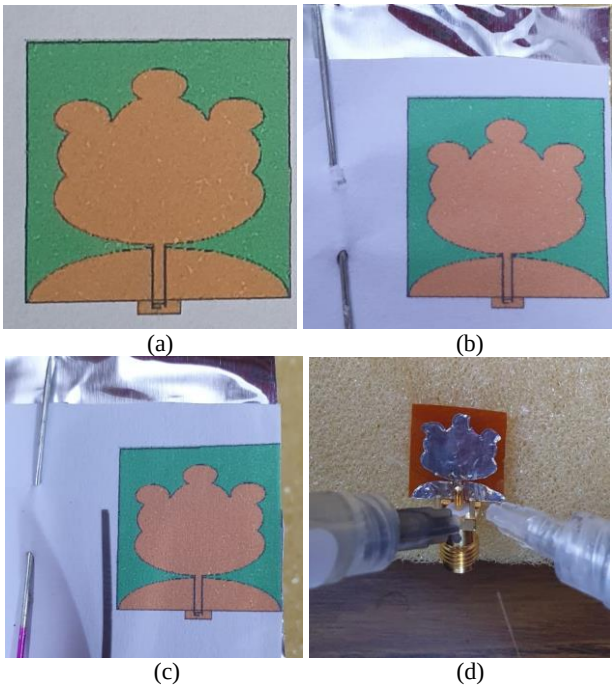

Fig.2. Fabrication process of the antenna: (a) step 1, (b) step 2, (c) step 3, (d) step 4

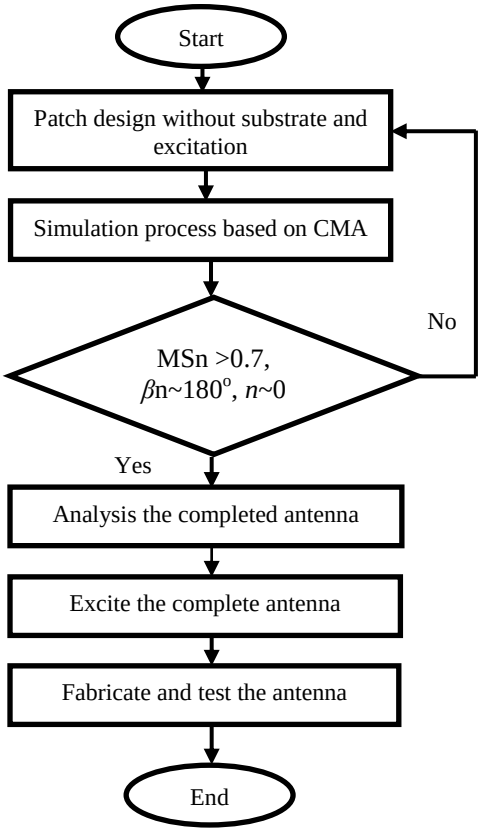

Fig.3. Workflow of the antenna design

III. Antenna Performance in Free Space

A. CMA Analysis

Three parameters of CMA, known as the modal significance (MSn), characteristic angle (βn), and eigenvalue (λn), are acquired. These characteristic attributes remain unaffected by the excitation or source. The comprehensive understanding of the characteristic mode theory can be found in the following equations:

$$\vec{J} = \sum_n a_n J_n \tag{1}$$

where J_n is the eigen current and a_n is the modal weighting coefficient.

$$a_n = \frac{V_n^i}{1 + j\lambda_n} \tag{2}$$

λ_n is the eigenvalue and V_n^i is the modal excitation coefficient.

$$MS_n = \left| \frac{1}{1 + j\lambda_n} \right| \tag{3}$$

where MS_n is the Modal significance.

$$\beta_n = 180 - \tan^{-1}(\lambda_n) \tag{4}$$

where β_n is the characteristic angle.

Modes with λn =0 indicating the externally resonant modes, while modes with λn > than 0 and λn < than 0 are called inductive and capacitive, respectively. On the other hand, the half power bandwidth of each CM is defined in the following equation:

$$BW = \frac{f_H - f_L}{f_{res}} \tag{5}$$

Where f_H, f_L, and f_{res} are the upper, lower half frequencies and resonant frequency, respectively. Based on equation (3), if λn=0 and MSn=1, then the associated mode is a resonant mode (f_{res}). If λn±1 and MSn=0.7, then the associated mode is the lower and upper frequency band mode (f_L and f_H), as follows:

$$MS(f_L) = MS(f_H) = \left| \frac{1}{1 + j\lambda_n} \right| = \frac{1}{\sqrt{2}} = 0.7 \tag{6}$$

Moreover, from equation (4), if λn = 0, the phase lag between the electric field and real current on the surface is 180° out of phase, and the mode is said to be the most effective radiating mode of the radiating element.

In this section, we will be analyzing the proposed antenna without a feeding structure based on the CM analysis using the FEKO simulator software. For our analysis, we will assume that the substrate and the ground plane are infinite in size. In most research papers, mode 1 is considered to be the dominant mode, which is primarily excited. Thus, this paper will highlight on these results. The modal significance of the proposed antenna in each iteration is shown in Fig. 4(a). It is worth mentioning that the lower frequency of the antenna gradually decreases as the number of iterations increases, ranging from 10.4 GHz to 9.25 GHz. The same behavior is observed for the plotted curve at the lower frequency when using the two other CMA parameters - characteristic angle and eigenvalue, as illustrated in Fig. 4(b) and (c) . These findings provide initial insight into the antenna's bandwidth during each iteration. As the number of fractal iterations increases, the lower frequency decreases while maintaining stability in the higher frequency. If the mode is correctly excited, it can be anticipated that the antenna's bandwidth will expand, which will be confirmed in the upcoming section.

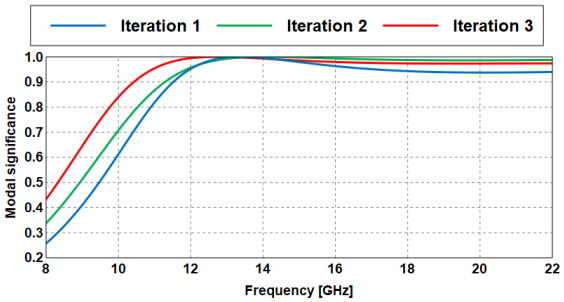

(a)

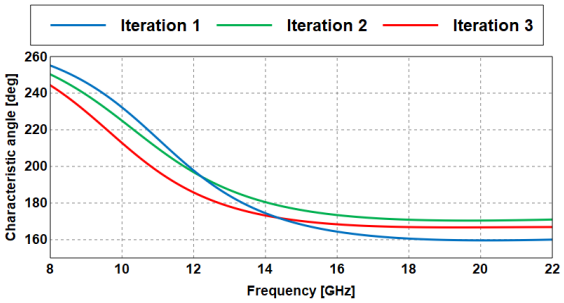

(b)

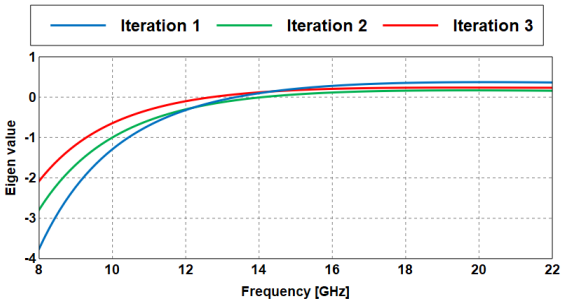

(c)

Fig.4. CMA parameters results – mode 1: (a) modal significance, (b) characteristic angle, (c): eigen value.

The distributions of surface currents on the xy-plane are displayed in Fig. 5 for frequencies of 14 GHz and 18 GHz. Throughout the three iterations, it is projected that electromagnetic waves are emitted from the border of the patch in the x-direction, with the currents primarily concentrated on the fractal side of the patch (upper side) at varying levels of intensity.

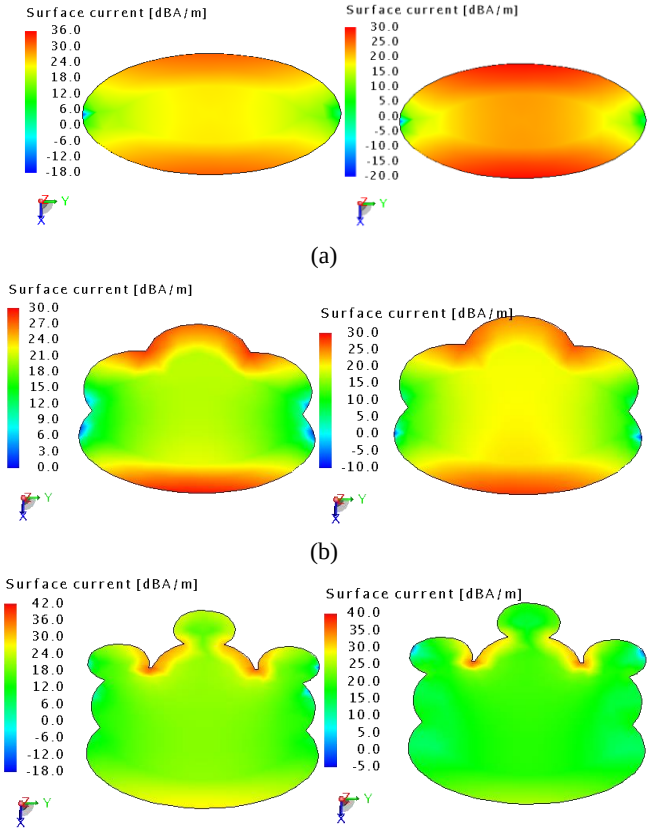

Fig.5. Modal current distribution – mode 1: (a) iteration 1, (b) iteration 2, (c) iteration 3, left (at 14 GHz), right (at 18 GHz).

B. Method of Moments (MoM) Analysis

Following the CMA analysis in the previous section, a complete antenna design was conducted. The analysis employed the common method of moments (MoM) through the use of the FEKO simulator software. In Fig. 6, the simulated results of the reflection coefficient are presented as a function of frequency. Upon the first iteration, the simulation results indicated that the antenna has an impedance bandwidth of 4.68 GHz, ranging from 13.16 GHz to 17.83 GHz. Subsequently, at iteration 2, the bandwidth was visibly expanded by 2.73 GHz, resulting in an operating band that spanned from 10.51 GHz to 17.93 GHz, achieving a total bandwidth of 7.41 GHz. Finally, during iteration 3, the bandwidth was further widened to 11.31 GHz, extending from 9.01 GHz to 20.31 GHz. Additionally, it is evident that the resonant frequency of the initial proposed antenna is 15.58 GHz. This frequency gradually increased to 15.71 GHz and 18.77 GHz during the second and third iterations, respectively. The last iteration resulted in a minimal dip in the magnitude of the reflection coefficient.

The simulated polar radiation patterns presented in Fig. 7(a-b) show the co and cross-polarization of the proposed antenna. The far field patterns across a spectrum of frequencies suggest that the antenna exhibited a quasi-omnidirectional pattern in the primary YOZ-plane (θ = 90^o), whilst a bidirectional radiation pattern is observed in the XOZ-plane (θ = 0^o).

The illustrated results in Fig. 8 depict the 2D cartesian plot of the simulated gains results.

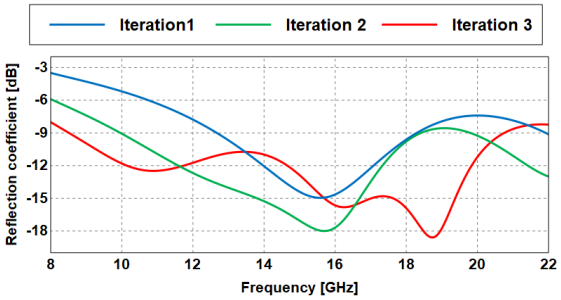

Fig.6. Reflection coefficient results of the proposed fractal antenna at the three iterations of design.

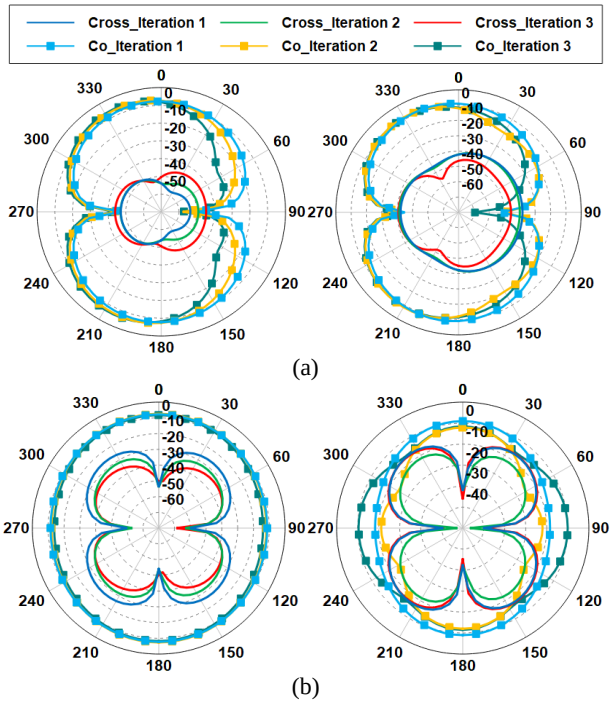

Fig.7. Simulated co-pol and cross-pol far-field pattern of the proposed fractal antenna (left): at 14 GHz (right): at 18 GHz: (a) Theta = 0 deg (XOZ plane), (b) Theta = 90 deg (YOZ plane)

At lower frequencies, the gain remains consistent at approximately 2.41 dBi for all iterations, gradually diminishing towards the upper frequencies within the range of 14 GHz to 20 GHz. Based on the simulation results in Fig. 9, the radiation efficiency ranges from 86% to 94%. Notably, the antennas proposed exhibit higher efficiencies at the lower frequencies within the obtained band, compared to the efficiencies observed at the higher frequencies.

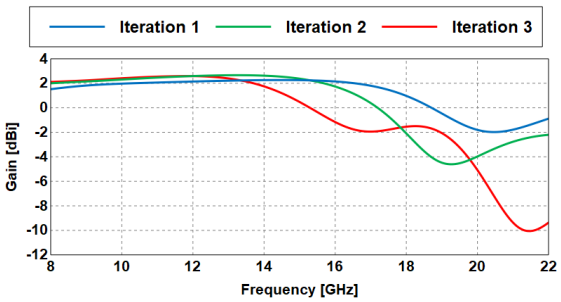

Fig.8. 2D cartesian plot represented the simulated gain results of the proposed antennas

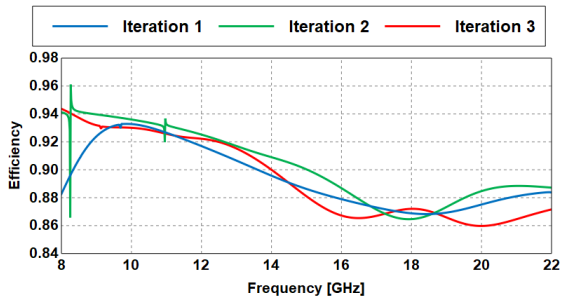

Fig.9. Simulated efficiency results of the proposed antennas

The radiation patterns of the simulated antenna in Fig. 10 are depicted in three-dimensional forms. It observes that the antenna attained a high gain of 5 dBi at 12 and 18 GHz. Furthermore, it retains a gain of 4 dBi at 14 and 16 GHz, respectively.

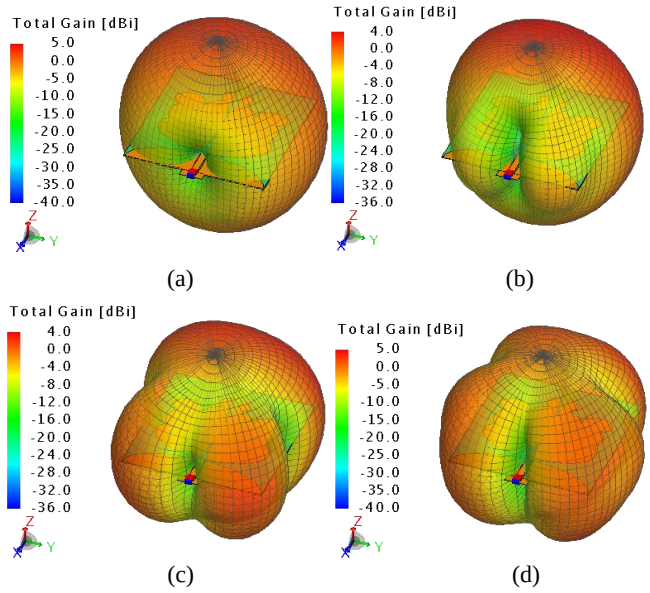

Fig.10. 3D total radiation pattern of the fractal antenna at: (a) 12 GHz, (b) 14 GHz, (c) 16 GHz, (d) 18 GHz

A summary of the comparison of the results illustrated in the Table 1.

TABLE 1
SUMMARY OF THE SIMULATED RESULTS OF FRACTAL ANTENNA IN THE LAST STEP OF ITERATION.

f (GHz)	Parameters		
	Reflection coefficient (dB)	2D-Gain (dBi)	Efficiency (%)
10	-11.83	2.41	93
12	-11.72	2.58	92
14	-11	1.75	90
16	-15.67	-1.16	87
18	-15.98	-1.55	87
20	-11.21	-5.08	86

The simulated and measured reflection coefficients in Fig. 11 exhibit close agreement, showcasing an impedance bandwidth of 11.3 GHz (9.01–20.31 GHz) and 10.28 GHz (9.17–19.45 GHz) respectively. The variation in bandwidth can be attributed to the utilization of a perfect substrate material in the simulations, which consequently has a significant impact on the measured results.

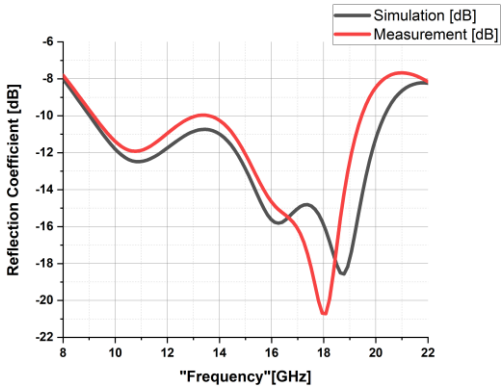

Fig.11. Simulated and measurement reflection coefficient of the cloud-fractal antenna

IV. CONCLUSION

This paper introduces a low-profile cloud-fractal design that enables a wideband patch antenna and operates from 9.01 GHz to 20.33 GHz, reaching up to 11.3 GHz. The radiator patch is analysed using the theory of characteristic modes as a starting point. The CMA approach is used to predict the antenna's bandwidth by estimating the variability obtained for the lower frequency at each iteration in the design process of the proposed fractal antenna. Subsequently, the overall antenna design demonstrates a peak gain of 5 dBi at 18 GHz. The proposed antenna is fabricated, and the measurement results show a satisfactory agreement with simulations in terms of reflection coefficients and bandwidth. Additionally, the antenna demonstrates both co and cross polarization of the radiation for E and H planes. The proposed cloud-fractal antenna demonstrates a reflection coefficient of less than -10 dB, offering a wider bandwidth and stable, satisfactory performance. It is capable of operating in three bands: X Band, Ku Band, and K Band.

REFERENCES

[1] M. Awais, A. Madni and W. T. Khan, "Design of a Compact High Isolation 4-Element Wideband Patch Antenna Array for GNSS Applications", in *IEEE Access*, vol. 10, pp. 13780-13786, 2022.

[2] X. Chen, L. Wang, D. Wu, J. Lei and G. Fu, "Compact and Wideband Directional Circularly Polarized Distributed Patch Antenna with High Efficiency", in *IEEE Access*, vol. 5, pp. 15942-15947, 2017.

[3] C. Zhao and C. -F. Wang, "Characteristic Mode Design of Wide Band Circularly Polarized Patch Antenna Consisting of H-Shaped Unit Cells", in *IEEE Access*, vol. 6, pp. 25292-25299, 2018.

[4] S. -K. Zhao, N. -W. Liu, Q. Chen, G. Fu and X. -P. Chen, "A Low-Profile Dielectric Resonator Antenna with Compact-Size and Wide Bandwidth by Using Metasurface", in *IEEE Access*, vol. 9, pp. 29819-29826, 2021.

[5] K. D. Xu, J. Zhu, S. Liao and Q. Xue, "Wideband Patch Antenna Using Multiple Parasitic Patches and its Array Application with Mutual Coupling Reduction", in *IEEE Access*, vol. 6, pp. 42497-42506, 2018.

[6] J. Sun and K. -M. Luk, "A Fully Transparent Wideband Water Patch Antenna with L-Shaped Feed", in *IEEE Open Journal of Antennas and Propagation*, vol. 2, pp. 968-975, 2021.

[7] R. Garbacz and R. Turpin, "A Generalized Expansion for Radiated and Scattered Fields", in *IEEE Transactions on Antennas and Propagation*, vol. AP-19, no. 3, pp. 348-358, May 1971.

[8] R. Harrington and J. Mautz, "Theory of Characteristic Modes for Conducting Bodies", in *IEEE Transactions on Antennas and Propagation*, vol. AP-19, no. 5, pp. 622_628, Sep. 1971.

[9] R. Harrington and J. Mautz, "Computation of Characteristic Modes for Conducting Bodies", in *IEEE Transactions on Antennas and Propagation*, vol. AP-19, no. 5, pp. 629_639, Sep. 1971.

[10] J. E. Bauer and P. K. Gentner, "Characteristic Mode Analysis of a Circular Polarised Rectangular Patch Antenna", in *Proc. 13th Eur. Conf. Antennas Propag. (EuCAP)*, Krakow, Poland, 2019 pp. 1-3.

[11] B. B. Q. Elias, P. J. Soh, A. A. Al-Hadi and P. Akkaraekthalin, "Gain Optimization of Low-Profile Textile Antennas using CMA and Active Mode Subtraction Method", in *IEEE Access*, vol. 9, pp. 23691-23704, 2021.

[12] Y. Shi, X. Zhang, Q. Qiu, Y. Gao and Z. Huang, "Design of Terahertz Detection Antenna with Fractal Butterfly Structure", in *IEEE Access*, vol. 9, pp. 113823-113831, 2021.

[13] F. Kazemi, "Dual Band Compact Fractal THz Antenna Based On CRLH-TL and Graphene Loads", in *Optik*, vol. 206, 2020.

[14] S.-H. Li and J.-S. Li, `"Smart Patch Wearable Antenna on Jeans Textile for Body Wireless Communication", in *Proc. 12th Int. Symp. Antennas, Propag. EM Theory (ISAPE)*, Hangzhou, China, Dec. 2018, pp. 1-4.

[15] N. Singh, V. Singh, R. Saini, J. P. Saini, and A. Bhoi, "Microstrip Textile Antenna with Jeans Substrate with Applications in S-band" in *Proc. Adv. Commun., Devices Netw*., Singapore, pp. 369-376, May 2018.

[16] A. Singh Saini, A. Sharma, P. Srivastava and K. Anjali, "Design of wideband Microstrip Antenna for X, Ku and K-Band applications," *2021 International Conference on Advance Computing and Innovative Technologies in Engineering (ICACITE)*, Greater Noida, India, 2021, pp. 723-725.

[17] R. Abirami, E. Gnanamanoharan, S. Sivagnanam and K. P. Priya, "Design of Compact Microstrip Patch Antenna for K Band and KU Band Applications," *2020 International Conference on System, Computation, Automation and Networking (ICSCAN)*, Pondicherry, India, 2020, pp. 1-7.

[18] M. El Jourmi, H. Ouahmane and F. Kharroubi, " Design and simulation of UWB Microstrip Patch Antenna for Ku/K Bands Applications," in *International Journal of Electrical and Computer Engineering*, vol. 9, pp. 4845- 4849, 2019.

[19] S. K. Dhakad and T. Bhandari, "A Hexagonal Broadband Compact Microstrip Monopole Antenna for C band, X Band and Ku Band Applications," *2017 International Conference on Computing, Communication and Automation (ICCCA)*, Greater Noida, India, 2017, pp. 1532-1536.

[20] F. Al-Janabi, M. Jit Singh, and A. Partap Singh Pharwaha, "Development of Microstrip Antenna for Satellite Application at Ku/Ka Band," *Journal of Communications*, vol. 16, no. 4, pp. 118-125, April 2021.